RNAi screen of *Salmonella* invasion shows role of COPI in membrane targeting of cholesterol and Cdc42

SUPPLEMENTARY INFORMATION

Supplementary figures S1-7

Supplementary table legends SI-V

Figure S1: Western blot verification of the depletion efficiency for key siRNAs used in secondary assays.

(A) Depletion of Actin-related protein 3 in HeLa cells decreased total Actr3 protein levels below the detection level for each of the 4 oligos tested (upper lane). Actin served as a loading control. **(B)** Depletion of Profilin-1 reduces the total Pfn1 protein levels significantly. Actin served as a loading control. **(C)** Densitometric analysis of Western blots confirming the siRNA mediated depletion efficiency of the targeted proteins. The depletion efficiency correlates with the effects of each oligo on the invasion efficiency of *S*. Typhimurium (SCV maturation assay) into these cells. These data confirms the specificity of the siRNA mediated depletion. The only exceptions were HS_COPG_6 and HS_ODC1_1, which may have resulted in off-target effects as indicated by reduced invasion efficiency without affecting the respective protein levels. This corresponds to 4.2% of all oligos tested.

Figure S2: Comparative depletion analysis yields equivalent phenotypes for five different subunits of the COPI complex.

HeLa cells were transfected with the indicated siRNAs. Binding, ruffling and SCV-maturation was analyzed (see Fig. 2A-C, Fig. 3A-D or Fig. 4A and B, respectively). The observed values were normalized to control siRNAs and depicted as the log2 of the relative effects.

Figure S3: Scatter plots identifying the step of *Salmonella* invasion affected by depletion of a host gene.

Relative effects on binding, ruffling and invasion are plotted against each other. Since the different steps of *Salmonella* Typhimurium invasion directly follow and depend on each other, an inhibitory effect on binding would also have an inhibitory effect on all subsequent steps of the invasion path (e.g. ruffling or invasion). Therefore, genes with a "pure" phenotype would appear along a line with a slope of 1 (blue area in the scheme on the right) or along the y-axis (light red shaded area). An additional inhibitory effect on the other step in invasion would place the genes in the purple area. The names of the tested genes are indicated in the color legend below the three graphs.

Figure S4: Rac1 is mislocalized after depletion of the COPI complex.

(A) Confocal images showing the distribution of Rac1-GFP in untreated cells (left), cells transfected with siRNA directed against *copG* (middle) or *copB1* (right). The intensity plots along the lines indicated in yellow are shown below the pictures. Scale bar: 10 μm **(B)** Quantification of the fold increase of the Rac1-GFP signal on the membrane compared to the cytosol. (*** = $p < 0.005$)

Figure S5: Cdc42, the sphingolipid GM1 and cholesterol are no longer localized to the plasma membrane after depletion of the COPI complex subunit CopG, while the cortical actin staining underneath the membrane remains unchanged.

Confocal images showing the distribution of actin (red), Cdc42 (green) and GM1 (blue) in non-treated cells **(A)** or in cells transfected with siRNA directed against *copG* **(B)**. Confocal images showing the distribution of actin (red), Cdc42 (green) and cholesterol (blue) in non-treated cells **(C)** or in cells transfected with siRNA directed

against *copG* **(D).** The intensity plots along the yellow lines are indicated in the respective color on the right site of the respective image sequence. Scale bar: 10 μm.

<u>Figure S6</u>: Rac1, the sphingolipid GM1 and cholesterol are no longer localized to the plasma membrane after depletion of the COPI complex subunit CopG, while the cortical actin staining underneath the membrane remains unchanged.

Confocal images showing the distribution of actin (red), Rac1 (green) and GM1 (blue) in non-treated cells **(A)** or in cells transfected with siRNA directed against *copG* **(B)**. Confocal images showing the distribution of actin (red), Rac1 (green) and cholesterol (blue) in non-treated cells **(C)** or in cells transfected with siRNA directed against *copG* **(D).** The intensity plots along the yellow lines are indicated in the respective color on the right site of the respective image sequence. Scale bar: 10 µm.

<u>Figure S7</u>: Rac1-enrichment is less pronounced upon COPI depletion.

(A) Confocal images showing the localization of Rac1-GFP in control cells (left) seeded one day prior to fixation in order to obtain separated cells and cells transfected with siRNA directed against *copG1* (right). The transfection protocol was identical as described for Figure 6. The top panels show typical cells (scale bar 10 µm), and the bottom panels display the analyzed area at higher magnification (scale bar 5 µm). The intensity plots along the lines indicated in yellow are shown below the pictures (left = outside of the cell → right = cytosol). The green or blue lines represent the intensities of Rac1-GFP fluorescence or CellMask staining, respectively. Cells expressing constitutively Rac1-GFP were stained with CellMask Membrane Stain (Invitrogen) at a concentration of 5 µg/ml for 5 min on ice prior to fixation. **(B)** Level of Rac1-GFP localization at the plasma membrane. The intensity ratio of the Rac1-GFP signal vs. the CellMask signal at the cell membrane was plotted. The calculation was performed as follows: The intensity values for both fluorophores were normalized to the brightest point along the line profile (lines were drawn in cell regions without visible membrane accumulations within the cell) and the position of the plasma membrane was determined by finding the brightest point on the line for the CellMask staining. The ratio of the signal at this point and a point located 4 pixels (0.5 µm) away within the cell was calculated for both fluorophores and the ratio of the Rac1-GFP signal to the CellMask signal was compared between control cells and cells transfected with siRNA directed against *copG* (** = $p < 0.005$; HS_CopG_7). At least 32 independent cells from two independent experiments were analyzed.

Legends for the supplementary tables

<u>Table SI</u>: Description of the different strains used in this study.

The name used in this work is indicated with "designation", the strain name used in other studies in "strain". The original genetic background for all constructed strains is SL1344.

<u>Table SII</u>: Data of the "druggable genome" screen.

The "druggable genome" siRNA library (Version 2.0) was obtained from Qiagen. HeLa cells were transfected with siRNA, infected with *S.* Tm^{SopE} (pM975) and the percentage of infected cells was calculated as described for Figure 1. Data for each well were subsequently normalized to the median of all siRNA on the plate and either expressed as log2 values (sheet "Log2 median") or Z-score corrected (sheet "Z-score corrected"). Experiments were done in triplicates; for each gene the median for each oligo (column "Oligo 1", "Oligo 2", "Oligo 3") and the median of all 3 oligos is indicated.

Table SIII: Effects of siRNAs on various steps of the *S.* Tm invasion process.

Data for *S.* Tm binding, effector injection, *S.* Tm-induced ruffling, membrane closure and SCV-maturation are reported in the respective Excel-sheets. The data for each gene and assay obtained by using the various oligos is indicated. In addition, the median of all 2 or 4 oligos are shown. P-values obtained by the Mann-Whitney U test with and without Benjamini Hochberg correction are also indicated. For each gene, Gene ID, NCBI gene symbol, name and sequence of siRNA oligos are given.

Table SIV: Classification of hits according to the specific step of *S.* Tm invasion

Data for the 60 strongest hits of the siRNA screen are shown. For these genes, data from 5 assays (binding, effector injection, ruffling, membrane closure, SCV-maturation) are available. For consistency, only those 2 oligos for which the complete data set was tested were considered. For each assay, the average effect of both oligos was calculated and is shown in the table. An increase of - 0.5 for an inhibiting hit and + 0.3 for a stimulating hit were chosen as thresholds. A gene was considered to participate in a specific step if the measured effect at this step exceeded the effect at all preceding steps of the *S.* Tm invasion cycle at least by this threshold. Two exceptions to these rules were necessary: 1) Changes beyond -4 were ignored (for instance the decrease from -4.3 for ruffling to -4.9 for invasion for ACTR3) since noise at such a low invasion level prohibits a precise measurement. 2) All stimulating 'membrane closure' hits were ignored. Stimulating effects on this invasion assay were consistently stronger than effects on ruffling or maturation. This is due to technical reasons. The number of intracellular bacteria which are quantified by this assay can increase without an upper limit in response to the knockdown of a gene. In contrast, the percentage of infected cells (which is quantified in the SCV maturation assay) is limited to 100%. Inhibiting and stimulating effects were color coded: Light green: partial positive effect. Dark green: full stimulating effect. Orange: partial inhibiting effect. Dark red: full inhibiting effect. Bright red: inhibiting effect at a third step. White: no effect. Grey: undecided.

Table SV: Overview of genes corresponding to their designated cluster.

Cluster analysis of the normalized step-specific phenotypes yielded 7 clusters. Genes and their corresponding clusters are shown.

A

B

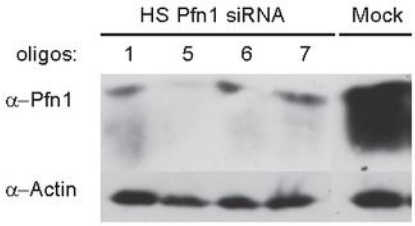

C

siRNA	relative invasion (log2)	depletion efficiency (%)
Hs_ACTR3_1	-5.0	100
Hs_ACTR3_5	-3.6	99
Hs_ACTR3_7	-5.1	100
Hs_ACTR3_8	-6.4	100
Hs_ATP1A1_5	-2.4	56
Hs_ATP1A1_6	-2.4	80
Hs_ATP1A1_7	-2.7	65
Hs_ATP1A1_8	-1.0	25
Hs_CDC42_7	-1.4	89
Hs_CDC42_8	-1.2	92
Hs_CDC42_10	-1.5	92
Hs_CDC42_12	-1.2	74
Hs_CFL1_1	0.9	98
HS_CFL1_3	0.4	98
HS_CFL1_6	1.0	98
HS_CFL2_5	0.5	98
Hs_COPB_5	-0.8	100
Hs_COPB_6	-2.1	100
Hs_COPB_8	-1.3	100
Hs_COPB_9	-4.3	100
Hs_COPG_1	-2.6	113
Hs_COPG_5	-2.9	118
Hs_COPG_6	-1.7	0
Hs_COPG_7	-3.0	105
Hs_ITGAV_2	0.4	98
Hs_ITGAV_3	0.3	77
Hs_ITGAV_6	0.1	7
Hs_ITGAV_7	0.9	104
Hs_NCKAP1_1	-1.6	96
Hs_NCKAP1_2	-2.2	87
Hs_NCKAP1_3	-2.5	92
Hs_NCKAP1_5	-2.3	91
Hs_ODC1_2	-1.1	50
Hs_ODC1_3	-0.9	30
Hs_ODC1_5	-0.3	0
Hs_ODC1_6	-1.4	9
Hs_PFN1_1	-1.5	59
Hs_PFN1_5	-3.0	85
Hs_PFN1_6	-2.2	76
Hs_PFN1_7	-2.4	68
Hs_RAB7_2	-0.2	66
Hs_RAB7_5	-0.6	100
Hs_RAB7_6	-1.4	100
Hs_RAB7_7	-0.8	100
Hs_RBX1_3	-2.9	80
Hs_RBX1_4	-1.8	90
Hs_RBX1_5	-1.8	88
Hs_RBX1_6	-2.7	96

Fig. S1

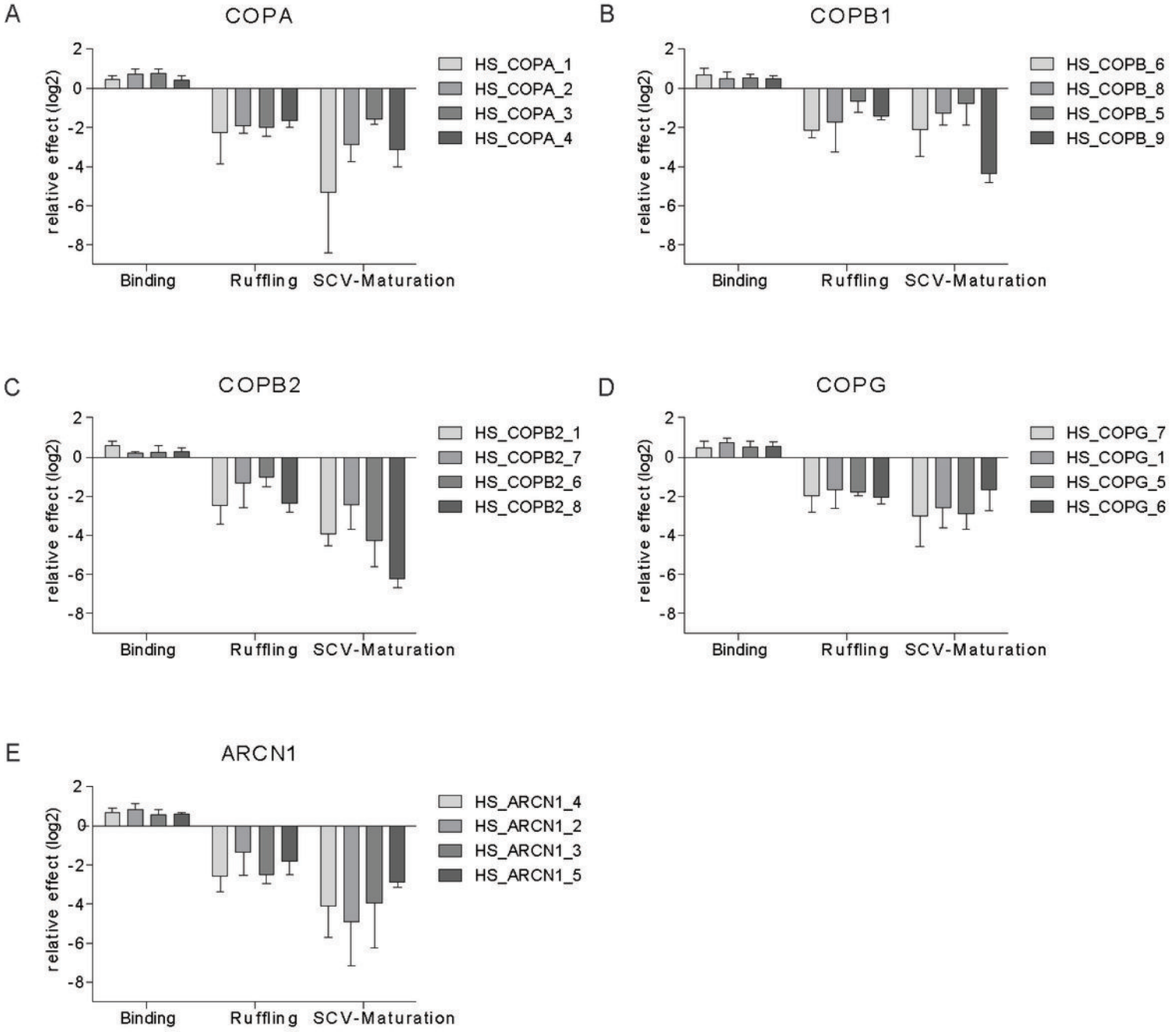
A
COPA
relative effect (log2)
2
0
-2
-4
-6
-8
Binding
Ruffling
SCV-Maturation
HS_COPA_1
HS_COPA_2
HS_COPA_3
HS_COPA_4
B
COPB1
HS_COPB_6
HS_COPB_8
HS_COPB_5
HS_COPB_9
C
COPB2
HS_COPB2_1
HS_COPB2_7
HS_COPB2_6
HS_COPB2_8
D
COPG
HS_COPG_7
HS_COPG_1
HS_COPG_5
HS_COPG_6
E
ARCN1
HS_ARCN1_4
HS_ARCN1_2
HS_ARCN1_3
HS_ARCN1_5

Fig. S2

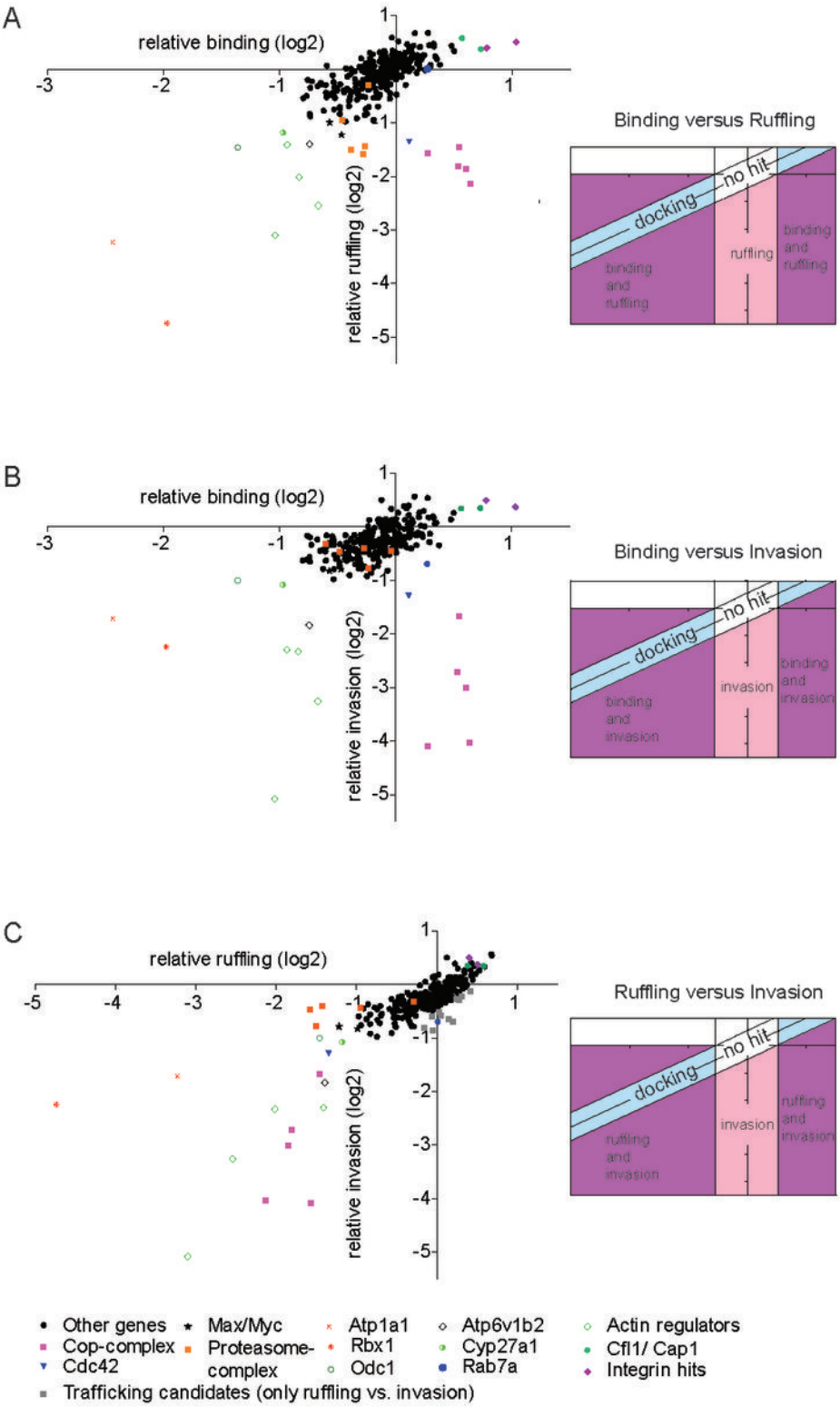
A
relative binding (log2)
relative ruffling (log2)
Binding versus Ruffling
docking
no hit
binding and ruffling
ruffling
binding and ruffling
B
relative binding (log2)
relative invasion (log2)
Binding versus Invasion
docking
no hit
binding and invasion
invasion
binding and invasion
C
relative ruffling (log2)
relative invasion (log2)
Ruffling versus Invasion
docking
no hit
ruffling and invasion
invasion
ruffling and invasion
Other genes
Max/Myc
Atp1a1
Atp6v1b2
Actin regulators
Cop-complex
Proteasome-complex
Rbx1
Cyp27a1
Cfl1/ Cap1
Cdc42
Odc1
Rab7a
Integrin hits
Trafficking candidates (only ruffling vs. invasion)

Fig. S3

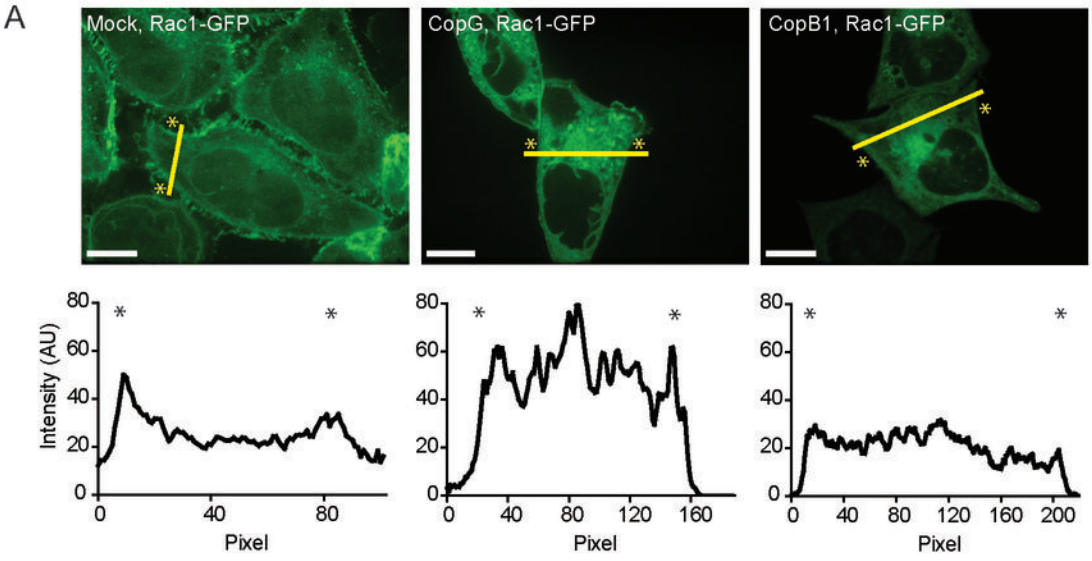
A
Mock, Rac1-GFP
CopG, Rac1-GFP
CopB1, Rac1-GFP
Intensity (AU)
Pixel
Pixel
Pixel

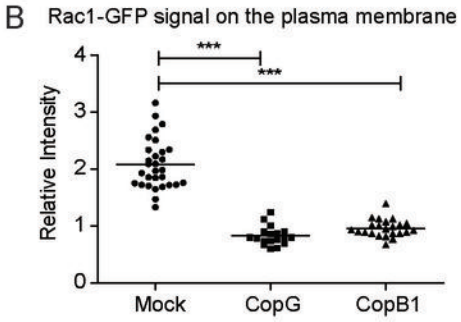
B
Rac1-GFP signal on the plasma membrane
Relative Intensity
***
***
Mock
CopG
CopB1

Fig. S4

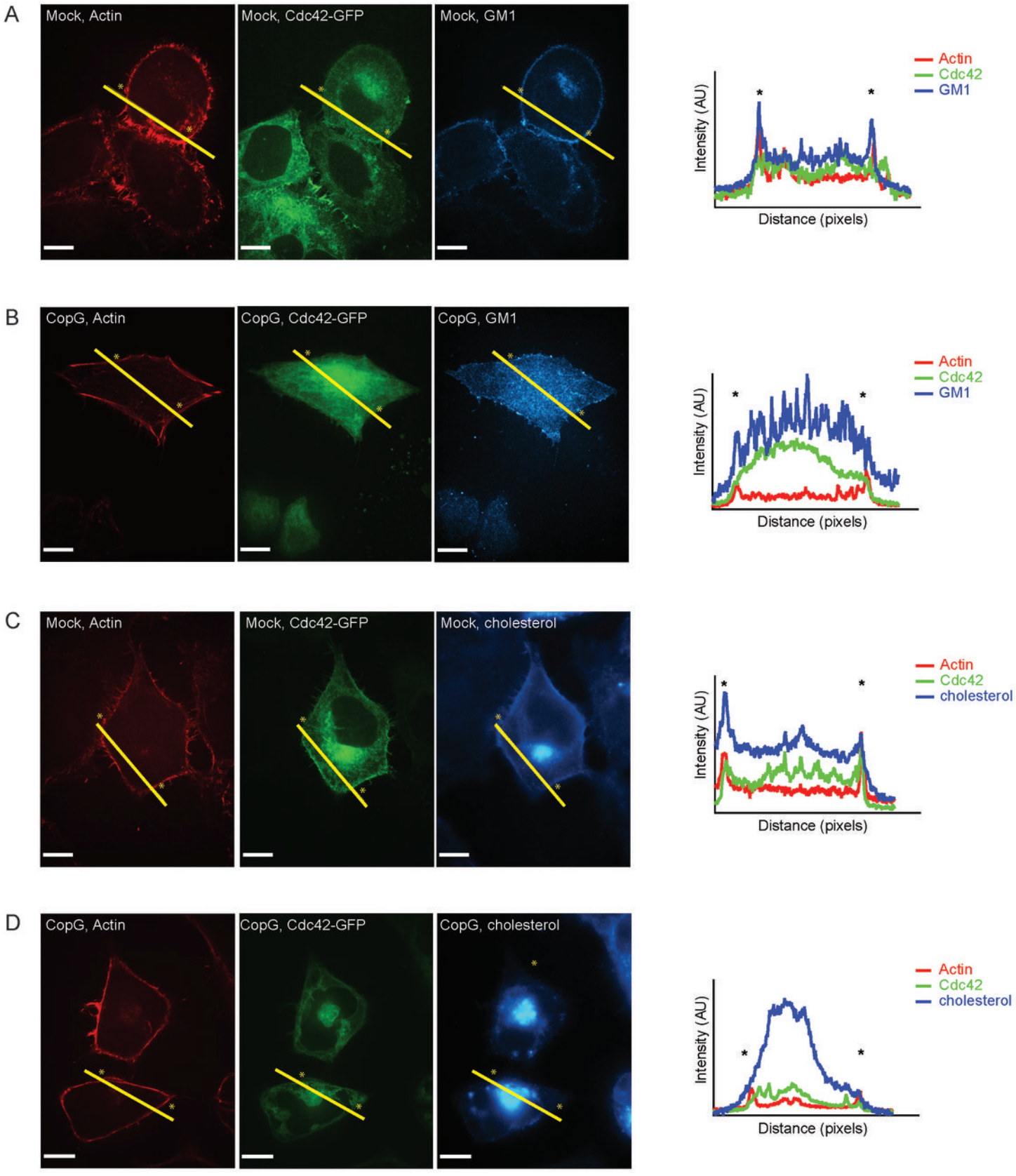
A
Mock, Actin
Mock, Cdc42-GFP
Mock, GM1
Actin
Cdc42
GM1
Intensity (AU)
Distance (pixels)
B
CopG, Actin
CopG, Cdc42-GFP
CopG, GM1
Actin
Cdc42
GM1
Intensity (AU)
Distance (pixels)
C
Mock, Actin
Mock, Cdc42-GFP
Mock, cholesterol
Actin
Cdc42
cholesterol
Intensity (AU)
Distance (pixels)
D
CopG, Actin
CopG, Cdc42-GFP
CopG, cholesterol
Actin
Cdc42
cholesterol
Intensity (AU)
Distance (pixels)

Fig. S5

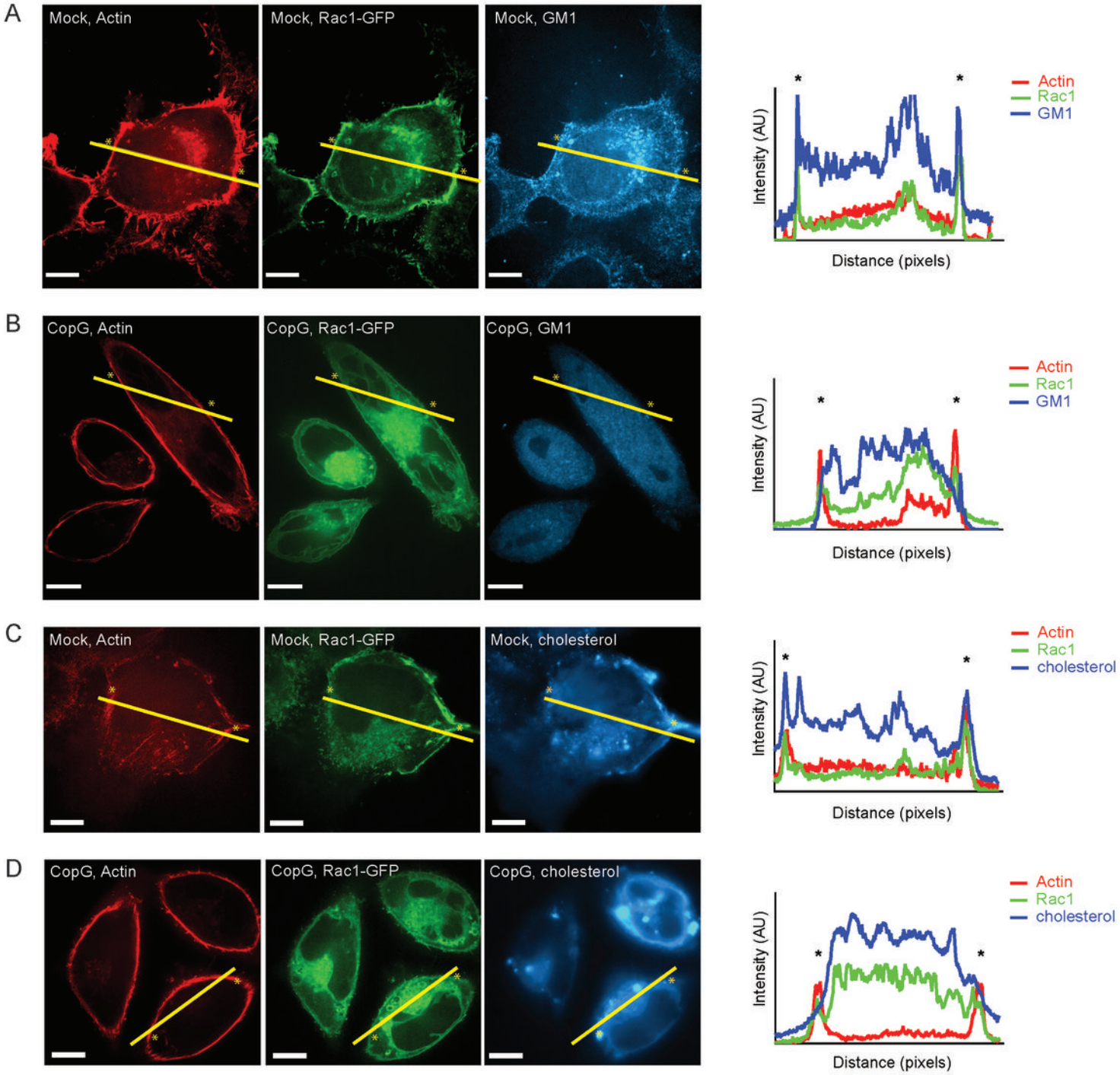
A
Mock, Actin
Mock, Rac1-GFP
Mock, GM1
Intensity (AU)
Distance (pixels)
Actin
Rac1
GM1
B
CopG, Actin
CopG, Rac1-GFP
CopG, GM1
Intensity (AU)
Distance (pixels)
Actin
Rac1
GM1
C
Mock, Actin
Mock, Rac1-GFP
Mock, cholesterol
Intensity (AU)
Distance (pixels)
Actin
Rac1
cholesterol
D
CopG, Actin
CopG, Rac1-GFP
CopG, cholesterol
Intensity (AU)
Distance (pixels)
Actin
Rac1
cholesterol

Fig. S6

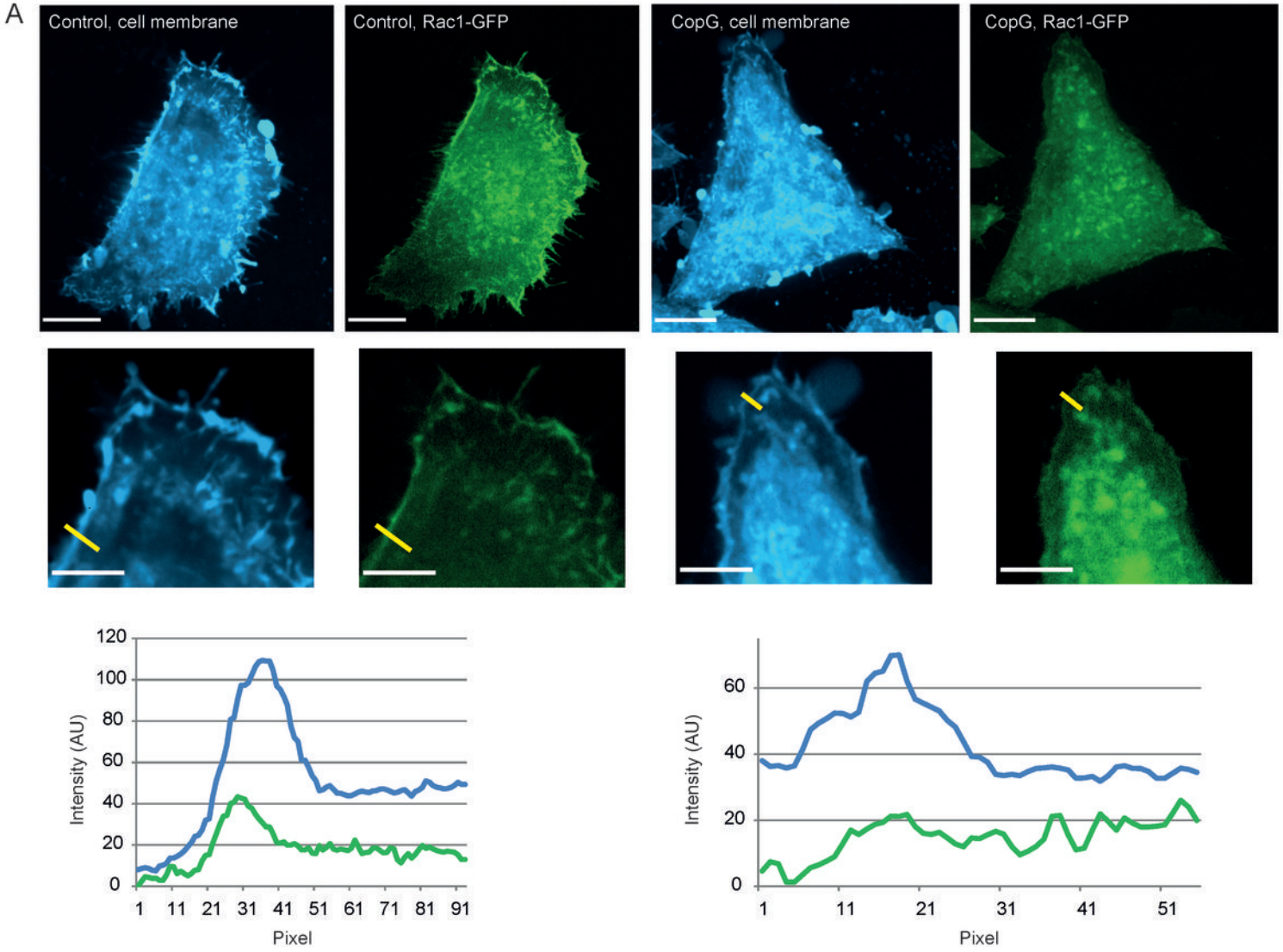
A
Control, cell membrane
Control, Rac1-GFP
CopG, cell membrane
CopG, Rac1-GFP
Intensity (AU)
Pixel
Intensity (AU)
Pixel

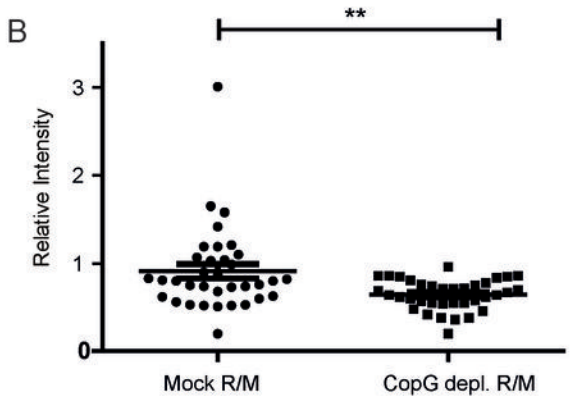
B
**
Relative Intensity
Mock R/M
CopG depl. R/M

Fig. S7

Suppl. Table SI

Designation	Strain	Genotype	Reference
S. Tm^{wt}	SB300	SL1344	(Hoiseth and Stocker, 1981)
S. Tm^{SopE}	M701	*ΔsopE2, sopB, sipA*	(Muller et al., 2009)
S. $Tm^{\Delta 4}$	M566	*ΔsopE, sopE2, sopB, sipA*	(Ehrbar et al., 2003)
S. $Tm^{\Delta T1}$	SB161	*ΔinvG*	(Kaniga et al., 1994)
S. $Tm^{SipA\text{-}TEM}$	M1128	*ΔsopE, sopE2, sopB; sipA-m45-BLA*	this study
S. $Tm^{\Delta T1\ SipA\text{-}TEM}$	M1114	*invC::aphT; sipA-BLA*	(Schlumberger et al., 2007)